Published in final edited form as:
Eur J Neurosci. 2012 October ; 36(7): 2906–2916. doi:10.1111/j.1460-9568.2012.08190.x.

Functional characterization of ether-a-go-go-related gene potassium channels in midbrain dopamine neurons: implications for a role in depolarization block

Huifang Ji[1,†], **Kristal R. Tucker**[2], **Ilva Putzier**[2], **Marco A. Huertas**[4], **John P. Horn**[3], **Carmen C. Canavier**[4], **Edwin S. Levitan**[2], and **Paul D. Shepard**[1]

[1]Department of Psychiatry and the Maryland Psychiatry Research Center, University of Maryland School of Medicine, Baltimore, Maryland 21228

[2]Department of Pharmacology and Chemical Biology, University of Pittsburgh, Pittsburgh, Pennsylvania 15261

[3]Department of Neurobiology, University of Pittsburgh, Pittsburgh, Pennsylvania 15261

[4]Department of Cell Biology and Anatomy and the Neuroscience Center of Excellence, LSU Health Sciences Center, 2020 Gravier Street, Suite D, New Orleans, LA, 70112, USA

Abstract

Bursting activity by midbrain dopamine neurons reflects the complex interplay between their intrinsic pacemaker activity and synaptic inputs. Although the precise mechanism responsible for the generation and modulation of bursting *in vivo* has yet to be established, several ion channels have been implicated in the process. Previous studies with nonselective blockers suggested that ether-a-go-go-related gene (ERG) K^+ channels are functionally significant. Here, electrophysiology with selective chemical and peptide ERG channel blockers (E-4031 and rBeKm-1) and computational methods were used to define the contribution made by ERG channels to the firing properties of midbrain dopamine neurons *in vivo* and *in vitro*. Selective ERG channel blockade increased the frequency of spontaneous activity as well as the response to depolarizing current pulses without altering spike frequency adaptation. ERG channel block also accelerated entry into depolarization inactivation during bursts elicited by virtual NMDA receptors generated with the dynamic clamp, and significantly prolonged the duration of the sustained depolarization inactivation that followed pharmacologically evoked bursts. *In vivo*, somatic ERG blockade was associated with an increase in bursting activity attributed to a reduction in doublet firing. Taken together, these results show that dopamine neuron ERG K^+ channels play a prominent role in limiting excitability and in minimizing depolarization inactivation. As the therapeutic actions of antipsychotic drugs are associated with depolarization inactivation of dopamine neurons and blockade of cardiac ERG channels is a prominent side effect of these drugs, ERG channels in the central nervous system may represent a novel target for antipsychotic drug development.

[†]Deceased Corresponding Author: Paul D. Shepard, Ph.D., Maryland Psychiatric Research Center, P.O. Box 21247, Baltimore, MD 21228. Fax: 410-402-6066, Pshepard@mprc.umaryland.edu.

Keywords

K_V11; hERG; KCNH2; bursting; antipsychotic drugs

Introduction

Midbrain dopamine (DA) neurons exhibit a continuum of patterned activity ranging from a tonic single-spike firing to a multiple-spike bursting discharge (Grace & Bunney, 1984a; Grace & Bunney, 1984b; Sanghera et al., 1984). Burst firing, which occurs in response to novel stimuli and has been implicated in some forms of reinforcement learning (Ljungberg et al., 1992; Montague et al., 1996; Pan et al., 2005; Roesch et al., 2007), is driven by changes in synaptic input and is strongly influenced by the intrinsic electrical properties of the DA neuron (Overton & Clark, 1997; Morikawa & Paladini, 2011).

A variety of voltage- and ligand-gated ion channels are thought to participate in the generation of DA cell bursting activity; these include NMDA receptors and L-type Ca^{2+} channels (Shepard & Stump, 1999; Morikawa *et al.*, 2003; Deister *et al.*, 2009; Putzier *et al.*, 2009a). Apamin-sensitive, small-conductance Ca^{2+}-activated K^+ (SK) channels have also been suggested to play a prominent role. Selective blockade of SK channels enhances NMDA-induced bursting *in vitro* (Johnson et al., 1992; Seutin et al., 1993) and increases the incidence and intensity of spontaneous bursting activity *in vivo* (Waroux *et al.*, 2005; Ji & Shepard, 2006). In brain slices, blockade of SK channels also results in a significant prolongation of an intrinsic pacemaker oscillation resulting in a plateau depolarization capable of driving the membrane into a temporary state of depolarization inactivation (Nedergaard *et al.*, 1993; Ping & Shepard, 1996; Johnson & Wu, 2004). Resumption of spontaneous firing occurs following repolarization of the plateau potential through a conductance mechanism that has yet to be identified.

A computational approach previously showed that the kinetics of an ether-a-go-go-related gene (ERG) potassium current (I_{ERG}) is suitable for terminating plateau potentials in DA neurons (Canavier et al., 2007). Genes encoding three distinct ERG channel subunits have been identified in mammalian brain, and moderate levels of the corresponding proteins are expressed in neurons within the ventral midbrain (Saganich et al., 2001; Papa et al., 2003). Although by no means selective, antipsychotic drugs capable of inducing depolarization block in DA neurons are also potent blockers of ERG K^+ channels (Kongsamut et al., 2002; Shepard et al., 2007). Haloperidol, which exhibits nanomolar affinity for the ERG channel (Ekins et al., 2002), prolongs plateau potentials in DA neurons (Canavier et al., 2007) and attenuates a slow, Ca^{2+}-independent afterhyperpolarization, which may be produced by an ERG K^+ current (Nedergaard, 2004). However, it remains unknown whether selective ERG channel blockers alter the activity of DA neurons in a manner consistent with their hypothesized role in modulating neuronal excitability.

Here, the role of ERG channels in regulating the excitability of midbrain DA neurons was determined with the use of mechanistically and structurally diverse selective ERG channel blockers *in vitro* and *in vivo*. E-4031 and the peptide recombinant BeKm-1 (rBeKm-1) reveal that ERG K^+ channels are active in the voltage range around firing threshold where

they play a prominent role in modulating neuronal excitability and in minimizing depolarization inactivation of spike-generating mechanisms in DA neurons.

Materials and methods

All experiments were performed using male Sprague–Dawley rats (Charles River, Wilmington, MA, USA or Hilltop Lab Animals, Scottdale, PA, USA). Animals were housed two per cage in a temperature-controlled vivarium under scheduled lighting conditions (12:12 h light:dark cycle) and provided with unrestricted access to food and water. All experiments were conducted with prior approval from the respective Institutional Animal Care and Use Committees at the University of Pittsburgh and the University of Maryland School of Medicine, and were performed in strict accordance with the procedures described in the *Guide for the Care and Use of Laboratory Animals (2010)*.

Current-clamp recording

DA neurons in the zona compacta of the substantia nigra or medial ventral tegmental area were identified by their electrophysiological characteristics and patchclamped as described previously (Ji et al., 2009). Briefly, rats (postnatal days 13–21) were anesthetized with chloral hydrate (400 mg/kg, i.p.) and decapitated, and the brain placed in ice-cold artificial cerebrospinal fluid (aCSF) consisting of (in mM) NaCl, 124; KCl, 4.0; NaH_2PO_4, 1.25; $MgSO_4$, 1.2; $NaHCO_3$, 25.7; $CaCl_2$, 2.45; ascorbate, 0.15; and glucose, 11; (pH 7.35, 295–305 mOsm). Coronal sections (250 μm) containing the substantia nigra were prepared using a vibrating tissue slicer and maintained in oxygenated aCSF at room temperature for a minimum of 1 hour. Whole slices were transferred to a recording chamber mounted on the stage of an Olympus BX51WI microscope and superfused (1.5 ml/min) with oxygenated aCSF maintained at 30°C. DA neurons were visualized at 40× using infrared differential contrast optics. Patch pipettes were prepared from standard-wall borosilicate tubing (1.5 mm OD; WPI, Sarasota, FL, USA) and filled with a solution containing (in mM): K-gluconate, 131; KCl, 9; HEPES, 20; EGTA, 0.1; Mg-ATP, 5; and GTP TRIS, 0.5 (pH 7.2, osmolarity 280–290 mOsm), giving a resistance of 8–18 MΩ. Electrodes were advanced under positive pressure and, on contact with a putative DA neuron, high-resistance seals were formed by application of negative pressure. The membrane was ruptured by suction and the membrane potential monitored using an Axoclamp 2B amplifier. Voltage recordings were digitized at 10 kHz using a laboratory interface and acquired with the PCLAMP software package (Molecular Devices, Sunnyvale, CA, USA). Timed current pulses were generated using a digital pulse generator and applied to the cell through the bridge circuit of the amplifier.

Dynamic-clamp recordings

Dynamic-clamp experiments were conducted as previously described (Putzier et al., 2009b). In brief, postnatal days 14–21 male Sprague–Dawley rats were anesthetized with isoflurane and decapitated. The brain was removed and placed in an ice-cold, sucrose-based aCSF containing (in mM): NaCl, 87; sucrose, 75; KCl, 2.5; $NaHCO_3$, 25; NaH_2PO_4, 1.25; $CaCl_2$, 0.5; $MgSO_4$, 7.0; glucose, 25; ascorbic acid, 0.15; and kynurenic acid, 1; pH 7.4, saturated with 95% O_2 and 5% CO_2. Coronal midbrain slices (250 μm) were cut with a vibratome

(Vibratome 3000; The Vibratome Company) in sucrose-based aCSF and then incubated in the same solution at room temperature for at least 1 h.

DA neurons were identified by location and electrophysiological characteristics, and patch-clamped as described previously (Putzier et al., 2009b). The patch-clamp pipette solution contained (in mM): potassium gluconate, 120; KCl, 20; HEPES, 10; $MgCl_2$, 2; EGTA, 0.1; and ATP, 1.2; pH 7.3. Oxygenated standard aCSF was used for bath perfusion at 2 ml/min and contained (in mM): NaCl, 124; KCl, 4; $NaHCO_3$, 25.7; NaH_2PO_4, 1.25; $CaCl_2$, 2.45; $MgSO_4$, 1.2; glucose, 11; and ascorbic acid, 0.15; pH 7.4. Whole-cell recordings were performed at 30–32°C, using an AM Systems 2400 amplifier in conjunction with the G-clamp dynamic-clamp system, as previously described (Kullmann et al., 2004; Putzier et al., 2009b). The conductance model for NMDA receptors [i.e., $I_{NMDA} = g_{NMDA} \times (V_m - E_{NMDA})/(1 + ([Mg^{2+}]_o/3.57) \times \exp(-V_m \times 0.062)]$ was based on Jahr & Stevens (1990), where the Mg^{2+} parameter was set to 1.4 mM and the reversal potential for NMDA (E_{NMDA}) was set to 0 mV. V_m was the instantaneous membrane potential, g_{NMDA} was the NMDA conductance to be added, and INMDA was the resulting instantaneous NMDA current to be injected. In dynamic-clamp experiments, 5–20 nS of g_{NMDA} was added to DA neurons. Then E-4031 dihydrochloride was superperfused over the slice at a rate of 2 ml/min for 8–10 minutes and the virtual NMDA conductance at which depolarization block first manifested under control conditions was reintroduced to the neuron.

Extracellular single-unit recording

Rats (300–350 g, postnatal days 60–75) were anesthetized with chloral hydrate (400 mg/kg, i.p.) and the soft tissue surrounding the ear canals and wound margins infiltrated with 2% mepivacaine before positioning the animal in a stereotaxic frame. Body temperature was maintained at 37 °C using a feedback-controlled heating pad. The scalp was incised and a burr hole drilled in the skull overlying the ventral midbrain. Recording electrodes were prepared from glass capillary tubing (1.5 mm OD; WPI) and filled with 0.5 M NaCl, or 0.5 M NaCl + 6 mM E-4031. Tips were broken back to achieve a final impedance of 4 – 6 MΩ *in vitro* and the electrodes positioned within the ventral midbrain (4.8 – 5.3 mm posterior from bregma, 1.2–2.5 mm lateral to the midline, 6.8 mm ventral to pial surface). Single-unit activity from well isolated cells was amplified, filtered (0.1 – 8 kHz bandpass) and monitored visually and aurally. Individual spikes were discriminated from background noise and digitized at 10 KHz using a laboratory interface and the Spike 2 software package (CED1401; CED, Cambridge, England). Cells were identified as dopaminergic based on their location and well-defined electrical characteristics including long duration (> 2.6 ms), triphasic action potentials, moderately slow firing rates (1–8 Hz) and irregular single-spike and burst-firing discharge patterns (Bunney et al., 1973; Wilson et al., 1977; Wang, 1981; Grace and Bunney, 1983).

E-4031 was applied locally to DA neurons by passive diffusion from recording electrodes as described previously (Steward et al., 1990; Tepper et al., 1995). Electrodes containing saline or saline + E4031 were used to record the activity of several DA neurons in each animal. To prevent contamination, three to five neurons were recorded using saline-filled electrodes prior to switching to drug-filled pipettes. Well isolated DA neurons were recorded for 10–15

minutes to establish their basal firing characteristics. Rate histograms were compiled in real time using a 10-s bin width. Interspike interval distributions were constructed off-line from 500 consecutive spikes and used to compute the coefficient of variation, an index of the regularity of neuronal firing. Spike trains were also analyzed for evidence of bursting activity as previously defined and validated (Grace & Bunney, 1984a). Briefly, burst initiation was defined as a spike pair with an interspike interval ≤ 80 ms. All subsequent spikes were considered part of the burst until an interval > 160 ms was encountered, which signaled burst termination. Unless otherwise indicated, spike doublets were included in the burst count. However, individual cells had to exhibit a minimum of three three-spike bursts in 500 consecutive events to be classified as a burst-firing neuron.

Drugs

N-[4-[[1-[2-(6-Methyl-2-pyridinyl)ethyl]-4-piperidinyl]carbonyl]phenyl]methanesulfonamide dihydrochloride (E-4031 dihydrochloride) was obtained from Tocris Cookson (Ellisville, MO, USA) prepared as a concentrated stock solution (10 mM) in deionized water. Individual aliquots of the stock were diluted in 0.5 mM NaCl or normal aCSF for use in the *in vivo* and *in vitro* recording studies, respectively. rBeKm-1 was obtained as a lyophilized powder from Alomone Labs (Jerusalem, Israel) and reconstituted in normal aCSF. R-N-(benzimidazol-2-yl)-1,2,3,4-tetrohydro-1-naphtylamine (NS8593) was obtained as a gift from NeuroSearch A/S (Ballerup, Denmark), dissolved in dimethylsulfoxide and diluted at least 1000-fold in normal aCSF prior to use. All other reagents were obtained from Sigma-Aldrich (St Louis, MO, USA).

Statistics

Unless otherwise indicated, all data are expressed as the arithmetic mean ± SEM. In some cases, the least-squares mean and corresponding SEM are provided. Drug and vehicle (control) responses were collected at approximately the same post-treatment interval (± 5 min). Omnibus testing was conducted using a Student's *t*-test or repeated-measures `ANOVA` (`RMANOVA`) unless the underlying assumptions of normality and equal variance were violated in which case the Wilcoxon signed-rank test was substituted. Single and multiple *post hoc* comparisons were made using the Bonferroni or Holm–Sidak method. All *post hoc* comparisons were two-sided at $\alpha = 0.05$.

Computational modeling

A schematic model was implemented in NEURON (Hines & Carnevale, 1997) and consisted of a soma with four dendrites that each branched once. All compartments had the same conductance densities for a constitutively active G-protein inwardly-rectifying K^+ conductance (Bradaia et al., 2009), a sodium leak (Khaliq & Bean, 2010), an L-type calcium conductance (Durante et al., 2004), a composite potassium conductance based on the composite from Ding et al. (2011a), a tetrodotoxin-sensitive sodium conductance (Seutin & Engel, 2010), an ERG conductance, a calcium-activated potassium conductance (Ping & Shepard, 1996) and an M-type potassium conductance (Drion et al.). A slow component of inactivation was added to the sodium channel per Ding et al. (2011a) and following Fernandez & White (2010). The ERG current is modeled as in Canavier et al. (2007) using a

three-state kinetic scheme (C↔O↔I) with transition rates adjusted to fit macroscopic current recordings from *Xenopus* oocytes expressing HERG channels (Ficker et al., 1998). Equations and parameters are given in the Supplementary Material.

Results

I_{ERG} affected pacemaker and evoked spiking activity

The functional effects of ERG channels in midbrain DA neurons were assessed using two structurally unrelated ERG K^+-channel blockers with disparate mechanisms of action. In the first set of experiments, cell-attached patch-clamp recording techniques were used to determine the effects of E-4031 (1–10 μM) and rBeKm-1 (50 nM) on the firing rate, discharge pattern and intrinsic oscillatory activity exhibited by DA neurons in brain slices. Addition of E-4031 to the tissue superfusion solution resulted in a concentration-dependent increase in neuronal firing rate (RMANOVA $F_{3,21} = 18.3$, $P < 0.001$, n=8; Fig. 1A–E). Maximal effects were observed in response to 3 μM E-4031 and resulted in a 56% increase in firing (range 12–107%; Fig. 1E). Nearly identical effects were obtained following bath application of rBeKm-1 at a concentration of 50 nM, which resulted in a 54% increase in firing rate (Paired t_7=−7.3, P< 0.001; range 21– 100%, n=8; Fig. 1F). The excitatory effects of ERG block on spontaneous activity were accompanied by an increase in the precision of firing as demonstrated by a reduction in the interspike interval coefficient of variation (Wilcoxon signed-rank test, $P < 0.05$; Fig. 1H). A similar trend was observed in response to E-4031 (RMANOVA $F_{3,21} = 2.6$, P=0.08; Fig. 1G). The effects of both ERG channel blockers were slow to develop, reaching a steady state after 15–20 minutes of continuous superfusion.

To further define the role of ERG K^+ channels in regulating the excitability of DA neurons, the number of spikes elicited by rectangular current pulses (0.05 – 0.2 nA, 1 sec duration) was compared before and after bath application of 50 nM rBeKm-1. Two-way RMANOVA revealed significant main effects for current intensity ($F_{3,21} = 148.9$, $P < 0.001$) and treatment ($F_{1,7}$ =6.6, P< 0.05; Fig. 2A). Although there was no evidence of a current × treatment interaction, a significant difference was observed in the average number of spikes elicited between control and rBeKm-1 treated cells (least-squares mean ± SEM: control, 4.6 ± 0.1 spikes; rBeKm-1, 5.1 ± 0.1 spikes; Holm–Sidak method, t=2.6, P <0.05). Additional evidence of an increase in neuronal excitability following ERG block was obtained by comparing the latency to onset of the first spike in trains of spikes evoked before and after rBeKm-1. As illustrated in Fig. 2C, rBeKm-1 (50 nM) decreased the interval between the onset of the current pulse and the occurrence of the first action potential in the train. The effect was most pronounced at 0.05 nA and diminished as the intensity of the stimulus current increased.

Trials in which depolarizing current steps evoked an identical number of spikes before and after rBeKm-1 provided an opportunity to assess the effects of ERG channel block on spike frequency adaptation. To isolate the effect of ERG on adaptation, the instantaneous frequency of consecutive spike pairs was expressed as a percentage of the maximal frequency and plotted as a function of its position in the train (Fig. 2B). Individual trials, comprised of between four and seven spikes obtained from six neurons, were used in this analysis. Although control and rBeKm-1 trials consisted of an identical number of spikes,

the average instantaneous frequency associated with the first several spikes evoked in rBeKm-1 was higher that associated with the corresponding spike pairs in control trials. Despite this early increase in neuronal excitability, blockade of ERG K^+ channels did not prevent the typical accommodation in firing frequency and by the third spike in the train both control and rBeKm-1-treated neurons were firing at essentially the same rate (spike positions 4 and 5, Fig. 2B).

This result was surprising given the excitatory effects of ERG blockade on basal firing rate. To gain insight into this observation, the role of ERG channels was examined in a model that recapitulated the role of ERG channels in pacemaker activity: eliminating g_{ERG} in the computational model resulted in a 50% increase in spontaneous activity. Furthermore, consistent with actual recordings from nigral brain slices, where input resistance measured at hyperpolarized potentials was not significantly changed by rBeKm-1 (control, 438 ± 26 MΩ; rBeKm-1, 50 nM, 468 ± 25 MΩ; paired t_7= −1.7, $P > 0.1$) or E-4031 (RMANOVA, $F_{3,21}$ =1.5, $P > 0.2$), the modeled ERG conductance made only a small contribution to the total somatic current at hyperpolarized potentials: in the model, the input resistance measured from −60 mV was 460 MΩ under control conditions (g_{ERG}=6 μS/cm^2) and 456 MΩ with the corresponding conductance g_{ERG} set to zero. The model also mimicked the limited effect of ERG channels on steady-state firing induced by sustained depolarization (i.e., as found above in Figure 2). Examination of the ERG conductance during modeled spike adaptation showed that, although I_{ERG} might be expected to summate at higher frequencies, ERG current actually comprises a smaller fraction of the total current at higher frequencies and thus the effect of ERG blockers on steady frequency decreases with increasing frequency. Thus, the effects of E-4031 and rBeKm-1 on pacemaker and evoked activity are consistent with the expected behavior of ERG channels.

I_{ERG} limited plateau oscillations

DA neurons *in vitro* exhibit an intrinsic oscillation in membrane potential that persists in the presence of tetrodotoxin (Fujimura & Matsuda, 1989; Harris *et al.*, 1989; Yung *et al.*, 1991; Kang & Kitai, 1993). Negative modulation of SK-type Ca^{2+}-activated K^+ channels changes the sinusoidal character of the oscillation, resulting in the appearance of a regenerative depolarizing plateau potential capable of driving a type of intrinsic bursting activity (Nedergaard *et al.*, 1993; Ping & Shepard, 1996; Ji *et al.*, 2009). In a previous study, we found that haloperidol, a potent ERG K^+ channel blocker and antipsychotic drug, significantly prolonged the plateau portion of the oscillation. These data, together with the established role of ERG K^+ channels in repolarizing cardiac plateau potentials, prompted us to assess the effects of E-4031 on regenerative plateau potentials in DA neurons in brain slices. Bath application of the negative SK channel modulator NS8593 (1–10 μM) resulted in the appearance of intrinsic bursting activity characterized by a group of closely spaced action potentials superimposed on a ramp-shaped depolarization that appeared to drive the neuron into a temporary state of depolarization block (Fig. 3A). Small-amplitude spikes were infrequently observed during the plateau phase of the oscillation. In 11 of 23 neurons tested, addition of E-4031 (10 μM) significantly increased the duration of the plateau (Fig. 3B), defined as the interval between the last full spike in the burst and the point at which the membrane potential crossed, and remained negative to, the value at the start of the plateau.

As a group, these cells showed an average increase of 90.7 ± 27% in the plateau duration (control, 2.3 ± 0.6 s; E-4031, 4.0 ± 0.9 s; paired t_9=-4.0, P=0.003). Only two cells were unaffected by the drug (<10% change). In the remaining 13 neurons, ERG block resulted in a sustained (> 2 min) depolarization and an attendant loss of spontaneous activity that appeared to be attributable to the induction of depolarization block. Figure 3D shows an example of one such cell in which the onset of spiking following a 20-minute superfusion with E-4031 resulted in the abrupt loss of spontaneous activity and a sustained membrane depolarization (Vm = −36 mV). Brief (200-ms) hyperpolarizing current pulses (Fig. 3D, lower trace, vertical arrows) triggered an abrupt repolarization of the membrane potential and a recommencement of spontaneous spiking that was again eliminated as the membrane was driven back into depolarization block. None of the cells that entered a persistent state of depolarization block recovered spontaneously.

I_{ERG} delayed NMDA-induced depolarization inactivation

Bursting activity in DA neurons depends on excitatory synaptic input, and loss of glutamatergic afferents is believed to be principally responsible for the absence of spontaneous bursting activity in brain slices (Overton & Clark, 1997). In an effort to assess the effects of ERG K^+ channel block on NMDA-mediated bursting, we employed a dynamic-clamp technique to simulate transient activation of these receptors *in vitro*. As previously reported (Putzier et al., 2009a), introduction of 20 nS of virtual NMDA current into a DA neuron evoked a burst of activity that rapidly drove the membrane into a state of depolarization inactivation (Fig. 4A). ERG channel blockade with 10 μM E-4031 significantly decreased the duration of spiking activity before the onset of depolarization block (Fig. 4B, E and G). However, the mean and peak firing frequencies were not significantly affected by E-4031 (peak frequency: control, 17.0 ± 2.25 Hz vs. E-4031, 18.2 ± 1.98 Hz, P = 0.614; mean frequency: control =, 11.1 ± 1.45 Hz vs. E-4031, 12.98 ± 1.57 Hz, P = 0.1959; n = 5) due to a concomitant decrease in the total number of spikes discharged prior to the cessation of spiking (Fig. 4F and H).

Nearly identical results were obtained in simulated voltage traces generated by our computational model. As illustrated in Fig. 4C, the model simulated the production of a burst of spikes as well as the subsequent induction of depolarization inactivation during a virtual pulse of NMDA conductance. Simulation of ERG block by reducing g_{ERG} to 0 reduced the duration of the burst without affecting spike frequency (Fig. 4D). These results suggest that ERG K^+ channels play a significant role in delaying the onset of NMDA-induced depolarization inactivation in DA neurons.

ERG block promoted burst firing *in vivo*

In the final group of experiments, extracellular single-unit recording techniques were used to determine the effects of local application of E-4031 to the soma on the activity of individual DA neurons in chloral hydrate-anesthetized rats. A total of 92 spontaneously active DA cells were sampled across the anteroposterior extent of the nucleus. Of these, 48 were recorded using saline-filled electrodes while the remaining 43 cells were recorded using pipettes containing saline + 6 mM E-4031. As illustrated in Fig. 5A, DA cells recorded using E-4031-containing electrodes were more likely to meet the operational definition of a

bursting discharge (40/43) than those recorded using saline-filled electrodes (30/48); χ^2 10.2, P=0.001). As a group, E-4031-treated cells fired faster (4.8 ± 0.3 Hz) than neurons sampled from the same rats using saline-filled electrodes (4.0 ± 0.2 Hz; t_{89}= 2.1, $P < 0.05$; Fig. 5B). This appeared to be due to the increased incidence of bursting activity among E-4031-treated cells as no differences were observed between the treatment groups when the comparison was limited to cells exhibiting a bursting discharge (control–burst firing only, 4.6 ± 0.3 Hz; E-4031–burst firing only, 4.9 ± 0.2 Hz; P = 0.4). The effects of E-4031 on firing rate and pattern did not change significantly during the course of the recording (Fig. 5B).

The ability of E-4031 to prolong the duration of plateau depolarizations *in vitro* suggested that local application of the drug to DA neurons *in vivo* might increase the number of spikes discharged per burst. However, as illustrated in Fig. 5C, the percentage of bursts comprised of between five and 10 spikes did not differ between groups of cells recorded using saline- and E-4031-filled electrodes. On the other hand, shorter bursts, consisting of three or four spikes, showed a trend toward an increased prevalence in E-4031 recordings; however, significant differences between treatment groups were limited to three-spike bursts (Students t_{68}= −2.533, P = 0.01). Interestingly, this trend was reversed among two-spike bursts, which were less prevalent in recordings made with E-4031-containing than saline-filled electrodes. Spike doublets or two-spike bursts were included in the burst count but, as noted earlier (see Materials and Methods), DA neurons were required to exhibit a minimum of three bursts in 500 consecutive events comprised of at least three spikes to be categorized as bursting. In agreement with previous reports, spike doublets were the most prevalent type of bursting activity in both control and E-4031 recordings, accounting for between 50 and 60% of the total number of bursting events. As illustrated in Fig. 5D, ~ 25% of the neurons recorded using saline-filled pipettes fired > 80% of their bursts as spike doublets. However, the incidence of these high doublet-firing cells was reduced by an order of magnitude in recordings obtained using E-4031-filled electrodes. These data suggest that the increased incidence of three-spike bursts following ERG block occurred at the expense of two-spike bursting. Given that this change in burst properties is subtle, the major role of somatic ERG channels *in vivo* is to control the incidence of bursting activity and mean frequency of activity (Fig. 5A and B).

Discussion

As intrinsic pacemakers, DA neurons retain the ability to fire spontaneously in the absence of synaptic input (Fujimura & Matsuda, 1989; Harris *et al.*, 1989; Yung *et al.*, 1991). When applied locally to DA neurons in brain slices, a preparation in which the majority of synaptic connections have been disrupted, E-4031 and rBeKm-1 significantly increased the rate of spontaneous firing. Both compounds are potent and selective ERG channel blockers; however, the molecular mechanisms underlying their effects on I_{ERG} are qualitatively different. E-4031 is a sulfonanilide antiarrhythmic drug with nanomolar affinity (IC_{50} ~250 nM) for the pore helix and acts from the cytoplasmic side of the membrane to preferentially block the channel in its open state (Kamiya et al., 2006; Vilums et al., 2011). The range of concentrations of E-4031 used in these experiments bracket those used in recent studies of I_{ERG} in other brain slice preparations (Pessia *et al.*, 2008; Hardman & Forsythe, 2009).

rBeKm-1 is 36-amino-acid peptide isolated from scorpion venom with low nanomolar affinity (IC_{50} ~3.3 nM) for the channel (Korolkova et al., 2001). The toxin acts from the extracellular side of the membrane and blocks the channel in its closed (resting) state. To the best of our knowledge, rBeKm-1 has not been used previously in a brain slice preparation. The concentration-dependent nature of the effect of E-4031 and the increased potency, but similar efficacy, of rBeKm-1 on DA cell activity are consistent with their pharmacodynamic properties at ERG K^+ channels, suggesting that actions of both drugs result from blockade of I_{ERG} as opposed to an unspecified action at another site. The ability of both blockers to increase spontaneous firing *in vitro* indicates that I_{ERG} is partially active during pacemaker firing and contributes to the resting discharge frequency. ERG currents in other neurons including the medial nucleus of the trapezoid body (Hardman & Forsythe, 2009) and medial vestibular nucleus (Pessia et al., 2008) are active at membrane potentials around firing threshold, and have been shown to contribute to the rate of spontaneous firing. Neither E-4031 nor rBeKm-1 altered input resistance; however, these measurements were made at membrane potentials well below firing threshold. Given that neither blocker altered the post-spike afterhyperpolarization, it seems likely that I_{ERG} slows pacemaker firing in DA neurons by partially opposing the inward currents leading to spike generation, a mechanism proposed to explain the excitatory effects of ERG blockers on other neurons (Pessia et al., 2008). Consistent with this interpretation, we also found that rBeKm-1 reduced the latency to the first spike evoked by rectangular current pulses, indicating that the depolarization preceding spike generation is sufficient to partially activate I_{ERG} in DA neurons.

Notably, ERG blockade did not result in a corresponding reduction in spike frequency adaptation akin to that observed in other preparations (Chiesa et al., 1997; Schonherr et al., 1999; Sacco et al., 2003; Pessia et al., 2008). In the present experiments, small current steps (< 0.2 nA) were used to maintain continuous spiking and to avoid depolarization block. As a result, the interspike interval was probably long enough to allow I_{ERG} to deactivate sufficiently to prevent the progressive increase in ERG current that mediates spike frequency adaptation in other neurons. Support for this interpretation was provided by modeling studies and experiments in which a dynamic-clamp technique was used to determine the effects of ERG block on NMDA receptor-induced bursting. As previously reported, introduction of a 20-nS NMDA conductance into the soma of midbrain DA neurons elicited a ‘burst’ of action potentials (Putzier et al., 2009a) with an average intraburst frequency > 10Hz. Spikes diminished in amplitude as the neuron was driven into a temporary state of depolarization block. In the presence of E-4031, the number of spikes per burst and the overall burst duration were significantly reduced; both effects are directly attributable to a more rapid induction of depolarization block. Nearly identical results were obtained from simulations of ERG block using a computational model of DA cell activity. In the model, depolarization block occurs during a virtual pulse of NMDA conductance because the additional depolarization prevents adequate removal of sodium channel inactivation. In a previously published study, we presumed that the fast component of sodium channel inactivation was responsible for entry into depolarization block (Kuznetsova et al., 2010). However, in our model, a slower component of recovery from inactivation played a larger role in the induction of depolarization block and the progressive reduction in spike amplitude that precedes it (Seutin & Engel, 2010; Ding *et al.*, 2011b). Thus, the ERG

conductance in DA neurons appears to provide an additional hyperpolarizing current during the interspike interval; this contributes to recovery from inactivation of the Na^+ current and delays the eventual entry into depolarization inactivation.

Additional evidence of a role for I_{ERG} in opposing depolarization block in DA neurons was obtained in experiments designed to assess the effects of E-4031 on intrinsic plateau oscillations. Under the recording conditions used in the present study, a reduction in SK current resulted in the appearance of a regenerative plateau oscillation capable of driving the cell into a transient state of depolarization block. In the absence of ERG channel blockers, the plateau phase of the oscillation was characterized by a slow hyperpolarizing drift that transitioned to rapid membrane repolarization. These observations are consistent with results from an earlier modeling study in which slow accumulation of I_{ERG} during the plateau potential was sufficient to trigger repolarization through voltage-dependent regenerative deactivation of an L-type calcium current (Canavier et al., 2007). Results showing that partial block of I_{ERG} by haloperidol prolongs the plateau are also consistent with the model which predicted that complete blockade of the conductance would result in persistent depolarization block. Consistent with these predictions, the majority of DA neurons exhibiting regenerative plateau oscillations showed sustained membrane depolarization and a concomitant loss of spontaneous activity in response to E-4031. The ability of brief hyperpolarizing current pulses to temporarily restore spiking indicates that the cessation of firing was due to depolarization block. Despite a near doubling in the duration of the plateau nearly 50% of the cells tested continued to oscillate in the presence of E-4031, indicating that other mechanisms are available to prevent sustained depolarization block. A variety of K^+ channels could subserve this function including another member of the ether-a-go-go family (EAG, Kv 10.1) refractory to the effects of E-4031 (Herzberg *et al.*, 1998; Ferreira *et al.*, 2012).

In the final group of experiments, local application of E-4031 was used to determine the effects of I_{ERG} blockade on spontaneous bursting activity *in vivo*. Although bursting in behaving animals is typically associated with an unexpected change in the sensorium, the majority of spontaneously firing DA neurons in anesthetized rats exhibit stochastic bursting activity (Grace & Bunney, 1984a). These bursts consist of two or more spikes superimposed on a depolarizing wave that extends beyond the last spike. The proportion of DA neurons exhibiting stochastic bursting (~60%) as well as the distribution of burst sizes in recordings obtained with saline-filled electrodes were similar to previous studies in chloral hydrate-anesthetized rats (Grace & Bunney, 1984a). By contrast, recordings obtained using pipettes containing E-4031 were characterized by a higher prevalence of bursting activity and an elevated mean firing rate. Bursting recorded using E-4031-filled electrodes was also comprised of fewer two-spike events and more three-spike bursts than comparable activity recorded with saline-filled electrodes. Given the ability of E-4031 to prolong the duration of intrinsic plateau depolarizations *in vitro*, it is conceivable that the modest increase in burst length observed *in vivo* derives from a prolongation of the depolarizing envelope associated with stochastic bursting and depolarization block *in vivo* (Grace & Bunney, 1984a; 1986).

The ability of DA neurons *in vivo* to fire spontaneously in the presence of locally applied E-4031 indicates that a reduction in somatic I_{ERG} does not result in an obligatory loss of

spontaneous activity. Although the incidence of spontaneously firing DA neurons did not appear to be reduced in recordings with E-4031-filled electrodes, the experimental design does not allow us to exclude the possibility that ERG blockade was effective in silencing some DA neurons *in vivo*. The extent of the diffusion of E-4031 from the recording pipette is also unknown and may have been insufficient to induce a complete ERG block throughout the dendritic tree. Nevertheless, the *in vitro* results show that ERG channels robustly oppose depolarization block, by both delaying its onset and shortening its duration. It is interesting to note in this regard that the majority of antipsychotic drugs capable of inducing depolarization block in DA neurons are potent ERG channel blockers (Kongsamut et al., 2002; Titier et al., 2004; Titier et al., 2005; Shepard et al., 2007; Valenti et al., 2011). Although the mechanisms contributing to these effects have yet to be determined, it is tempting to speculate that the ERG-blocking capabilities of these drugs may be involved. The utility of ERG channels as potential therapeutic targets recently received further support from studies showing that genetic variation in the expression of a unique human ERG channel isoform modulates the response of patients with schizophrenia to antipsychotic drugs (Huffaker et al., 2009; Apud et al., 2011).

Supplementary Material

Refer to Web version on PubMed Central for supplementary material.

Acknowledgments

We are grateful to Dr Sonia Gasparini for helpful discussions of the data and computational modeling. This work was supported by PHS Grants R01NS061097 (C.C.C.) and 1F32NS078994 (K.R.T). This manuscript is dedicated to the memory of our deceased colleague Dr Huifang Ji.

Abbreviations

aCSF	artificial cerebrospinal fluid
DA	dopamine
ERG	ether-a-go-go-related gene
$\boldsymbol{I_{ERG}}$	ERG potassium current
NS8593	R-N-(benzimidazol-2-yl)-1,2,3,4-tetrohydro-1-naphtylamine
rBeKM-1	recombinant BeKm-1
RMANOVA	repeated-measures ANOVA
SK	small-conductance Ca^{2+}-activated K^+

References

Apud, JA.; Zhang, F.; Decot, H.; Bigos, KL.; Weinberger, DR. Society for Neuroscience Meeting Society for Neuroscience. Washington, DC: 2011. Genetic variation in KCNH2 associated with expression in brain of a unique hERG isoform modulates antipsychotic response in patients with schizophrenia; p. CC14

Bradaia A, Trube G, Stalder H, Norcross RD, Ozmen L, Wettstein JG, Pinard A, Buchy D, Gassmann M, Hoener MC, Bettler B. The selective antagonist EPPTB reveals TAAR1-mediated regulatory

mechanisms in dopa-minergic neurons of the mesolimbic system. Proc Natl Acad Sci U S A. 2009; 106:20081–20086. [PubMed: 19892733]

Canavier CC, Oprisan S, Callaway J, Ji H, Shepard PD. Computational model predicts a role for ERG current in repolarizing plateau potentials in dopa-mine neurons: implications for modulation of neuronal activity. J Neurophysiol. 2007; 98:3006–3022. [PubMed: 17699694]

Chiesa N, Rosati B, Arcangeli A, Olivotto M, Wanke E. A novel role for HERG K+ channels: spike-frequency adaptation. J Physiol. 1997; 501(Pt 2):313–318. [PubMed: 9192303]

Deister CA, Teagarden MA, Wilson CJ, Paladini CA. An intrinsic neuronal oscillator underlies dopaminergic neuron bursting. J Neurosci. 2009; 29:15888–15897. [PubMed: 20016105]

Ding S, Matta SG, Zhou FM. Kv3-like potassium channels are required for sustained high-frequency firing in basal ganglia output neurons. J Neurophysiol. 2011a; 105:554–570. [PubMed: 21160004]

Ding S, Wei W, Zhou FM. Molecular and functional differences in voltage-activated sodium currents between GABA projection neurons and dopamine neurons in the substantia nigra. J Neurophysiol. 2011b; 106:3019–3034. [PubMed: 21880943]

Drion G, Bonjean M, Waroux O, Scuvee-Moreau J, Liegeois JF, Sejnowski TJ, Sepulchre R, Seutin V. M-type channels selectively control bursting in rat dopaminergic neurons. Eur J Neurosci. 31:827–835. [PubMed: 20180842]

Durante P, Cardenas CG, Whittaker JA, Kitai ST, Scroggs RS. Low-threshold L-type calcium channels in rat dopamine neurons. J Neurophysiol. 2004; 91:1450–1454. [PubMed: 14645383]

Ekins S, Crumb WJ, Sarazan RD, Wikel JH, Wrighton SA. Three-dimensional quantitative structure-activity relationship for inhibition of human ether-a-go-go-related gene potassium channel. J Pharmacol Exp Ther. 2002; 301:427–434. [PubMed: 11961040]

Fernandez FR, White JA. Gain control in CA1 pyramidal cells using changes in somatic conductance. J Neurosci. 2010; 30:230–241. [PubMed: 20053905]

Ferreira NR, Mitkovski M, Stuhmer W, Pardo LA, Del Bel EA. Ether-ago-go 1 (Eag1) Potassium Channel Expression in Dopaminergic Neurons of Basal Ganglia is Modulated by 6-Hydroxydopamine Lesion. Neurotox Res. 2012; 21:317–333. [PubMed: 22048886]

Ficker E, Jarolimek W, Kiehn J, Baumann A, Brown AM. Molecular determinants of dofetilide block of HERG K+ channels. Circ Res. 1998; 82:386–395. [PubMed: 9486667]

Fujimura K, Matsuda Y. Autogenous oscillatory potentials in neurons of the guinea pig substantia nigra pars compacta in vitro. Neurosc Lett. 1989; 104:53–57.

Grace AA, Bunney BS. The control of firing pattern in nigral dopamine neurons: burst firing. J Neurosci. 1984a; 4:2877–2890. [PubMed: 6150071]

Grace AA, Bunney BS. The control of firing pattern in nigral dopamine neurons: Single spike firing. J Neurosci. 1984b; 4:2866–2876. [PubMed: 6150070]

Grace AA, Bunney BS. Induction of depolarization block in midbrain dopamine neuron by repeated administration of haloperidol: analysis using in vivo intracellular recording. J Pharmacol and Exp Therapeut. 1986; 238:1092–1100.

Hardman RM, Forsythe ID. Ether-a-go-go-related gene K+ channels contribute to threshold excitability of mouse auditory brainstem neurons. J Physiol. 2009; 587:2487–2497. [PubMed: 19359372]

Harris NC, C W, Greenfield SA. A possible pacemaker mechanism in pars compacta neurons of the guinea-pig substantia nigra revealed by various ion channel blocking agents. Neuroscience. 1989; 31:355–362. [PubMed: 2552348]

Herzberg IM, Trudeau MC, Robertson GA. Transfer of rapid inactivation and sensitivity to the class III antiarrhythmic drug E-4031 from HERG to M-eag channels. J Physiol. 1998; 511(Pt 1):3–14. [PubMed: 9679158]

Hines ML, Carnevale NT. The NEURON simulation environment. Neural Comput. 1997; 9:1179–1209. [PubMed: 9248061]

Huffaker SJ, Chen J, Nicodemus KK, Sambataro F, Yang F, Mattay V, Lipska BK, Hyde TM, Song J, Rujescu D, Giegling I, Mayilyan K, Proust MJ, Soghoyan A, Caforio G, Callicott JH, Bertolino A, Meyer-Lindenberg A, Chang J, Ji Y, Egan MF, Goldberg TE, Kleinman JE, Lu B, Weinberger DR. A primate-specific, brain isoform of KCNH2 affects cortical physiology, cognition, neuronal repolarization and risk of schizophrenia. Nat Med. 2009; 15:509–518. [PubMed: 19412172]

Jahr CE, Stevens CF. Voltage dependence of NMDA-activated macroscopic conductances predicted by single-channel kinetics. J Neurosci. 1990; 10:3178–3182. [PubMed: 1697902]

Ji H, Hougaard C, Herrik KF, Strobaek D, Christophersen P, Shepard PD. Tuning the excitability of midbrain dopamine neurons by modulating the Ca2+ sensitivity of SK channels. Eur J Neurosci. 2009; 29:1883–1895. [PubMed: 19473240]

Ji H, Shepard PD. SK Ca2+-activated K+ channel ligands alter the firing pattern of dopamine-containing neurons in vivo. Neuroscience. 2006; 140:623–633. [PubMed: 16564639]

Johnson SW, Seutin V, North RA. Burst firing in dopamine neurons induced by N-methyl-D-aspartate: Role of electrogenic sodium pump. Science. 1992; 258:665–667. [PubMed: 1329209]

Johnson SW, Wu YN. Multiple mechanisms underlie burst firing in rat midbrain dopamine neurons in vitro. Brain Res. 2004; 1019:293–296. [PubMed: 15306267]

Kamiya K, Niwa R, Mitcheson JS, Sanguinetti MC. Molecular determinants of HERG channel block. Mol Pharmacol. 2006; 69:1709–1716. [PubMed: 16474003]

Kang Y, Kitai ST. Calcium spike underlying rhythmic firing in dopaminergic neurons on the rat substantia nigra. Neurosci Res. 1993; 18:195–207. [PubMed: 7907413]

Khaliq ZM, Bean BP. Pacemaking in dopaminergic ventral tegmental area neurons: depolarizing drive from background and voltage-dependent sodium conductances. J Neurosci. 2010; 30:7401–7413. [PubMed: 20505107]

Kongsamut S, Kang J, Chen XL, Roehr J, Rampe D. A comparison of the receptor binding and HERG channel affinities for a series of antipsychotic drugs. Eur J Pharmacol. 2002; 450:37–41. [PubMed: 12176106]

Korolkova YV, Kozlov SA, Lipkin AV, Pluzhnikov KA, Hadley JK, Filippov AK, Brown DA, Angelo K, Strobaek D, Jespersen T, Olesen SP, Jensen BS, Grishin EV. An ERG channel inhibitor from the scorpion Buthus eupeus. J Biol Chem. 2001; 276:9868–9876. [PubMed: 11136720]

Kullmann PH, Wheeler DW, Beacom J, Horn JP. Implementation of a fast 16-Bit dynamic clamp using LabVIEW-RT. J Neurophysiol. 2004; 91:542–554. [PubMed: 14507986]

Kuznetsova AY, Huertas MA, Kuznetsov AS, Paladini CA, Canavier CC. Regulation of firing frequency in a computational model of a midbrain dopaminergic neuron. J Comput Neurosci. 2010; 28:389–403. [PubMed: 20217204]

Ljungberg T, Apicella P, Schultz W. Responses of monkey dopamine neurons during learning of behavioral reactions. J Neurophysiol. 1992; 67:145–163. [PubMed: 1552316]

Montague PR, Dayan P, Sejnowski TJ. A framework for mesencephalic dopamine systems based on predictive Hebbian learning. J Neurosci. 1996; 16:1936–1947. [PubMed: 8774460]

Morikawa H, Khodakhah K, Williams JT. Two intracellular pathways mediate metabotropic glutamate receptor-induced Ca2+ mobilization in dopamine neurons. J Neurosci. 2003; 23:149–157. [PubMed: 12514211]

Morikawa H, Paladini CA. Dynamic regulation of midbrain dopamine neuron activity: intrinsic, synaptic, and plasticity mechanisms. Neuroscience. 2011; 198:95–111. [PubMed: 21872647]

Nedergaard S. A Ca2+-independent slow after hyperpolarization in substantia nigra compacta neurons. Neuroscience. 2004; 125:841–852. [PubMed: 15120845]

Nedergaard S, Flatman JA, Engberg I. Nifedipine- and omega-conotoxin-sensitive Ca2+ conductances in guinea-pig substantia nigra pars compacta neurones. J Physiol. 1993; 466:727–747. [PubMed: 8410714]

Overton PG, Clark D. Burst firing in midbrain dopaminergic neurons. Brain Res Rev. 1997; 25:312–334. [PubMed: 9495561]

Pan WX, Schmidt R, Wickens JR, Hyland BI. Dopamine cells respond to predicted events during classical conditioning: evidence for eligibility traces in the reward-learning network. J Neurosci. 2005; 25:6235–6242. [PubMed: 15987953]

Papa M, Boscia F, Canitano A, Castaldo P, Sellitti S, Annunziato L, Taglialatela M. Expression pattern of the ether-a-gogo-related (ERG) K+ channel-encoding genes ERG1, ERG2, and ERG3 in the adult rat central nervous system. J Comp Neurol. 2003; 466:119–135. [PubMed: 14515244]

Pessia M, Servettini I, Panichi R, Guasti L, Grassi S, Arcangeli A, Wanke E, Pettorossi VE. ERG voltage-gated K+ channels regulate excitability and discharge dynamics of the medial vestibular nucleus neurons. J Physiol. 2008; 586(Pt 20):4877–4890. [PubMed: 18718985]

Ping HX, Shepard PD. Apamin-sensitive Ca^{2+}-activated K^{+} channels regulate pacemaker activity in nigral dopamine neurons. Neuroreport. 1996; 8:809–814. [PubMed: 8733751]

Putzier I, Kullmann PH, Horn JP, Levitan ES. Cav1.3 channel voltage dependence, not Ca2+ selectivity, drives pacemaker activity and amplifies bursts in nigral dopamine neurons. J Neurosci. 2009a; 29:15414–15419. [PubMed: 20007466]

Putzier I, Kullmann PH, Horn JP, Levitan ES. Dopamine neuron responses depend exponentially on pacemaker interval. J Neurophysiol. 2009b; 101:926–933. [PubMed: 19073798]

Roesch MR, Calu DJ, Schoenbaum G. Dopamine neurons encode the better option in rats deciding between differently delayed or sized rewards. Nat Neurosci. 2007; 10:1615–1624. [PubMed: 18026098]

Sacco T, Bruno A, Wanke E, Tempia F. Functional roles of an ERG current isolated in cerebellar Purkinje neurons. J Neurophysiol. 2003; 90:1817–1828. [PubMed: 12750425]

Saganich MJ, Machado E, Rudy B. Differential expression of genes encoding subthreshold-operating voltage-gated K+ channels in brain. J Neurosci. 2001; 21:4609–4624. [PubMed: 11425889]

Sanghera MK, Trulson ME, German DC. Electrophysiological properties of mouse dopamine neurons: in vivo and in vitro studies. Neuroscience. 1984; 12:793–801. [PubMed: 6472621]

Schonherr R, Rosati B, Hehl S, Rao VG, Arcangeli A, Olivotto M, Heinemann SH, Wanke E. Functional role of the slow activation property of ERG K+ channels. Eur J Neurosci. 1999; 11:753–760. [PubMed: 10103069]

Seutin V, Engel D. Differences in Na+ conductance density and Na+ channel functional properties between dopamine and GABA neurons of the rat substantia nigra. J Neurophysiol. 2010; 103:3099–3114. [PubMed: 20357070]

Seutin V, Johnson SW, North RA. Apamin increases NMDA-induced burst-firing of rat mesencephalic dopamine neurons. Brain Res. 1993; 630:341–344. [PubMed: 8118703]

Shepard PD, Canavier CC, Levitan ES. Ether-a-go-go-related gene potassium channels: What's all the buzz about? Schizophr Bull. 2007; 33:1263–1269. [PubMed: 17905786]

Shepard PD, Stump D. Nifedipine blocks apamin-induced bursting activity in nigral dopamine-containing neurons. Brain Res. 1999; 817:104–109. [PubMed: 9889338]

Steward O, Tomasulo R, Levy WB. Blockade of inhibition in a pathway with dual excitatory and inhibitory action unmasks a capability for LTP that is otherwise not expressed. Brain Res. 1990; 516:292–300. [PubMed: 2364294]

Tepper JM, Martin LP, Anderson DR. GABAA receptor-mediated inhibition of rat substantia nigra dopaminergic neurons by pars reticulata projection neurons. J Neurosci. 1995; 15:3092–3103. [PubMed: 7722648]

Titier K, Canal M, Deridet E, Abouelfath A, Gromb S, Molimard M, Moore N. Determination of myocardium to plasma concentration ratios of five antipsychotic drugs: Comparison with their ability to induce arrhythmia and sudden death in clinical practice. Toxicol Appl Pharmacol. 2004; 199:52–60. [PubMed: 15289090]

Titier K, Girodet PO, Verdoux H, Molimard M, Begaud B, Haverkamp W, Lader M, Moore N. Atypical antipsychotics: from potassium channels to torsade de pointes and sudden death. Drug Saf. 2005; 28:35–51. [PubMed: 15649104]

Valenti O, Cifelli P, Gill KM, Grace AA. Antipsychotic drugs rapidly induce dopamine neuron depolarization block in a developmental rat model of schizophrenia. J Neurosci. 2011; 31:12330–12338. [PubMed: 21865475]

Vilums M, Overman J, Klaasse E, Scheel O, Brussee J, Ijzerman AP. Understanding of molecular substructures that contribute to hERG K(+) channel blockade: synthesis and biological evaluation of E-4031 analogues. ChemMed-Chem. 2011; 7:107–113.

Waroux O, Massotte L, Alleva L, Graulich A, Thomas E, Liegeois JF, Scuvee-Moreau J, Seutin V. SK channels control the firing pattern of midbrain dopaminergic neurons in vivo. Eur J Neurosci. 2005; 22:3111–3121. [PubMed: 16367777]

Yung WH, Hausser MA, Jack JJB. Electrophysiology of dopaminergic and non-dopaminergic neurones of the guinea-pig substantia nigra pars compacta in vitro. J Physiol. 1991; 436:643–667. [PubMed: 2061849]

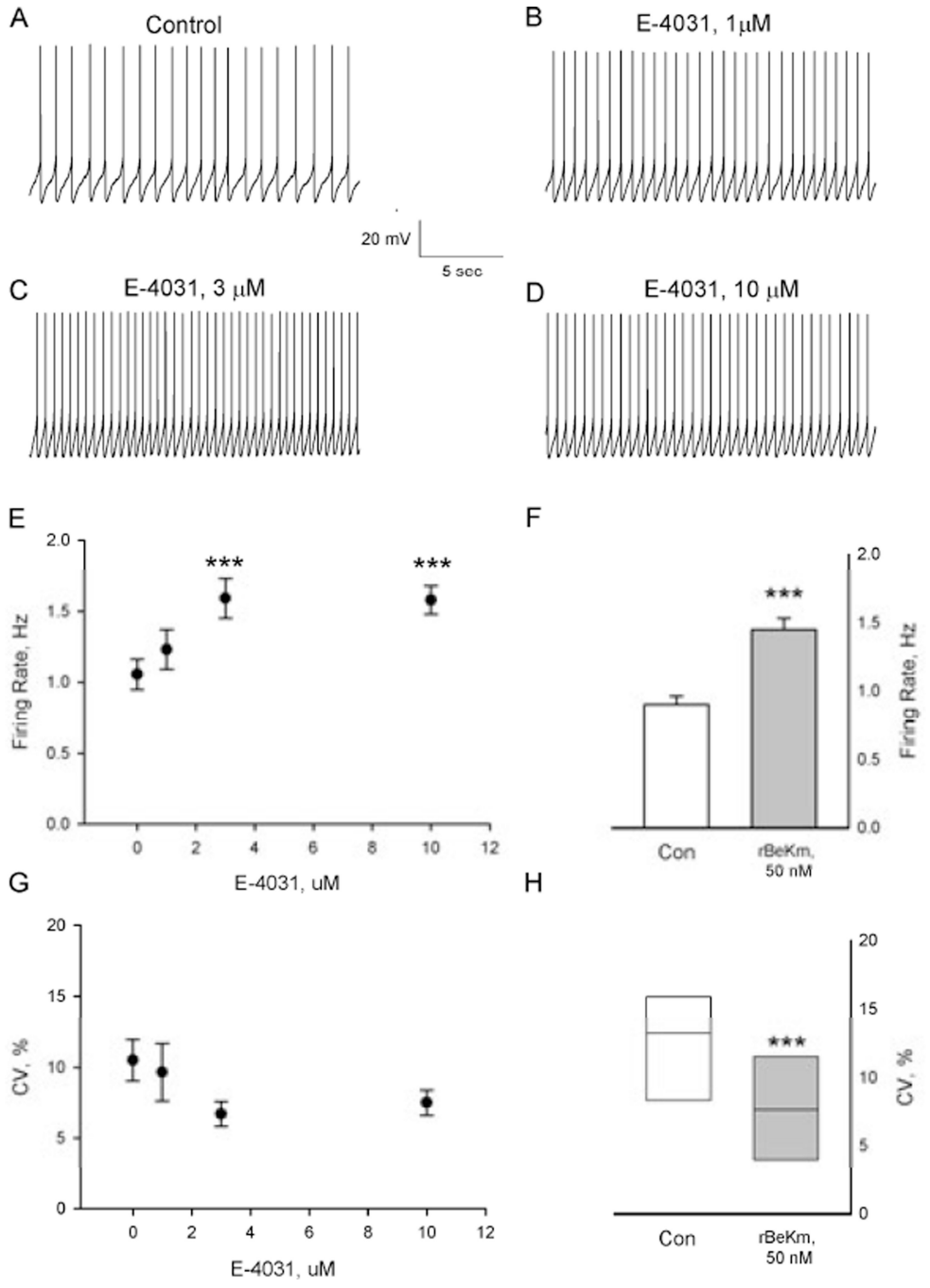

Figure 1.

Blockade of ERG K^+ channels increased the firing rate of DA-containing neurons in brain slices. (A–D) Representative tracings from a spontaneously active DA neuron treated with increasing concentrations of E-4031 (1–10 μM). All records are from the same cell. (E) Summary of the effects of cumulative administration of E-4031 on DA cell firing rate. Each point represents the mean ± SEM of n=8 neurons. *P < 0.001 vs. control (Bonferroni t test). (F) Bath application of rBeKm-1 (50 nM) significantly increased the activity of DA neurons (***P < 0.001, paired t-test, n=8). (G and H) Effects of (G) E-4031 and (H) rBeKm-1 on the

interspike interval coefficient of variation. The horizontal line within the box plots indicates the median value while the upper and lower limits of the box denote the 75th and 25th quartiles, respectively. ***$P < 0.05$, Wilcoxon signed-rank test.

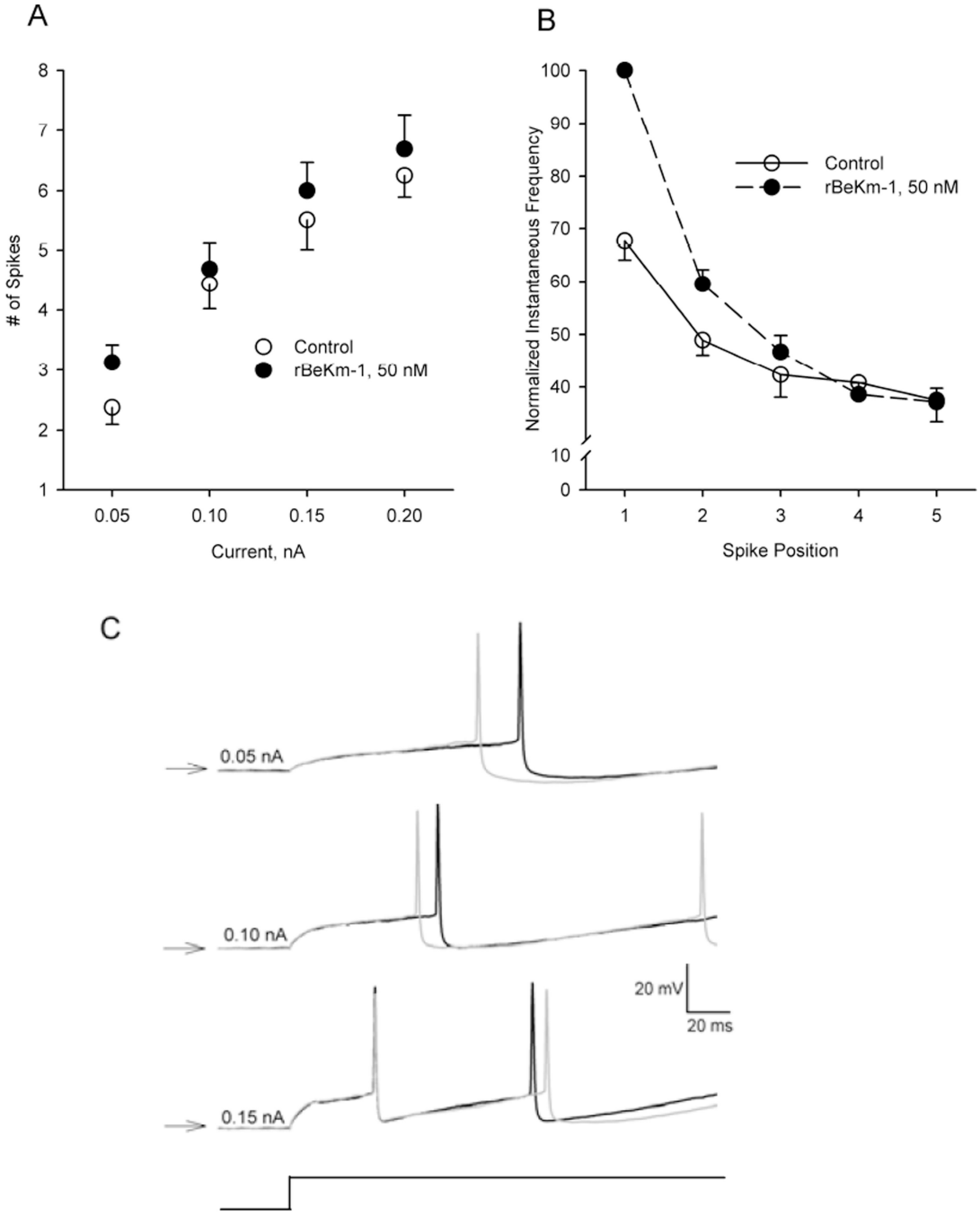

Figure 2.

Effects of ERG K^+ channel block on DA cell excitability *in vitro*. (A) Effects of rBeKm-1 on the number of spikes elicited by 1-sec depolarizing current pulses of increasing intensity (0.05–0.2nA). (B) Effects of rBeKm-1 on the slow adaptation in firing frequency observed during depolarizing current steps. Vertical axis, instantaneous firing rate expressed as a percentage of the cell's maximal response (typically the first spike pair in the presence of rBeKm-1). Horizontal axis, position of the spike pair in the train. (C) Representative example of the effects of rBeKm-1 50 nM, gray traces, on latency to the first spike elicited

by a 1-s current pulse of increasing amplitude (0.05, 0.10 and 0.15 nA). All recordings were obtained from the same cell. Onset of the current pulse is illustrated in the lower trace (current monitor). Horizontal arrows, −60 mV

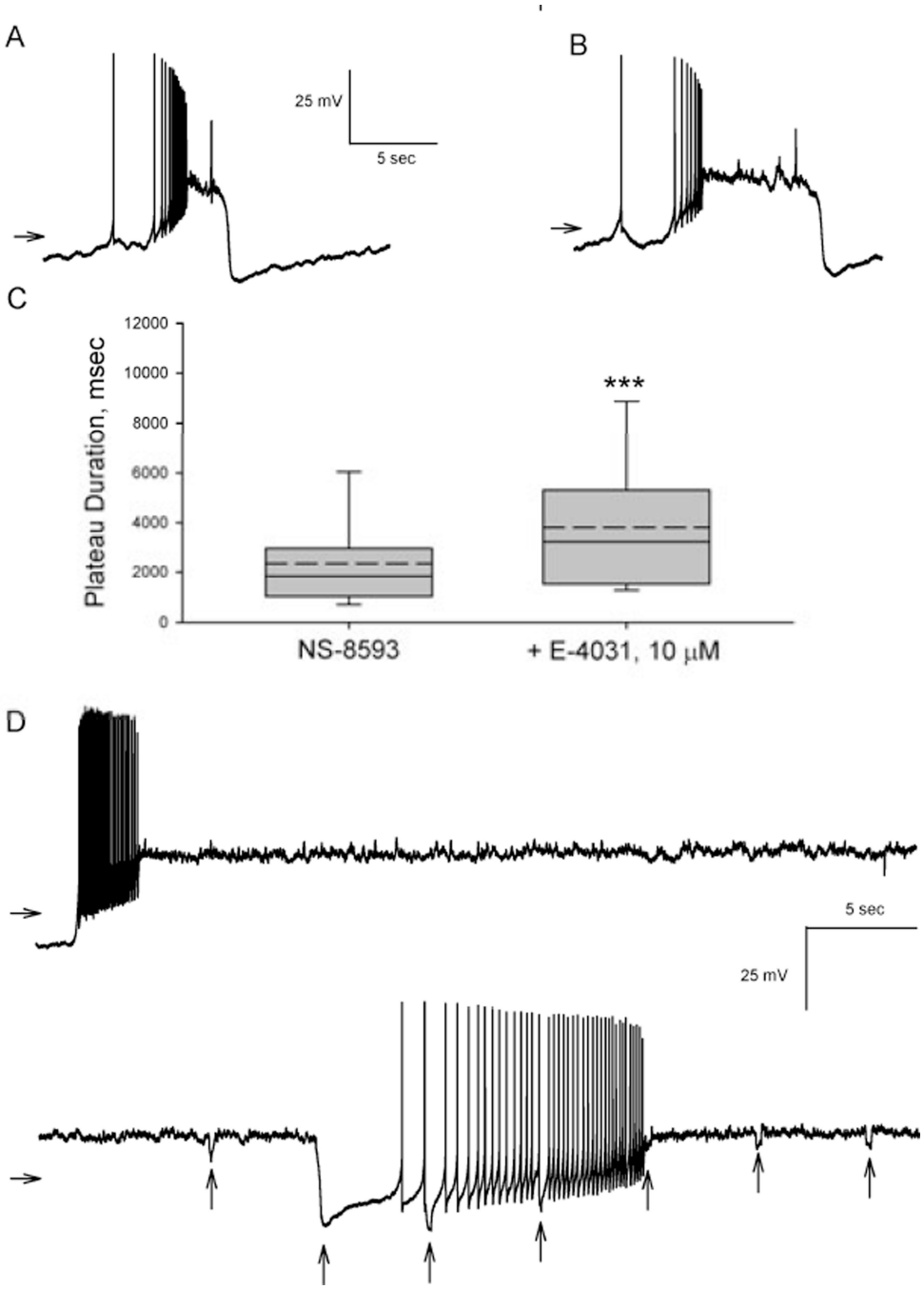

Figure 3.

ERG K^+ channel block prolonged plateau potentials induced by the SK-channel negative modulator, NS8593. (A) Representative tracing from a DA neuron in the presence of NS8593 (6 μM). Note the 'burst' of action potentials elicited during the initial phase of a depolarizing plateau potential. (B) Addition of E-4031 (10 μM) prolongs the duration of the plateau. (C) Box (25th and 75th percentiles) and whisker (10th and 90th percentiles) plot illustrating the effects of E-4031 (10 μM) on the duration of spontaneous plateau potentials elicited by negative modulation of SK channels. Solid and dashed lines inside the box

represent the median and mean, respectively. ***$P < 0.003$ vs. NS8593. (D) Superfusion with E-4031 (10 μM) resulted in the loss of spontaneous activity through depolarization block following removal of a negative bias current. Brief hyperpolarizing current pulses (0.03 nA, 200 ms; vertical arrows) were capable of repolarizing the neuron which led to recovery of spontaneous spiking followed by the rapid return of depolarization block.

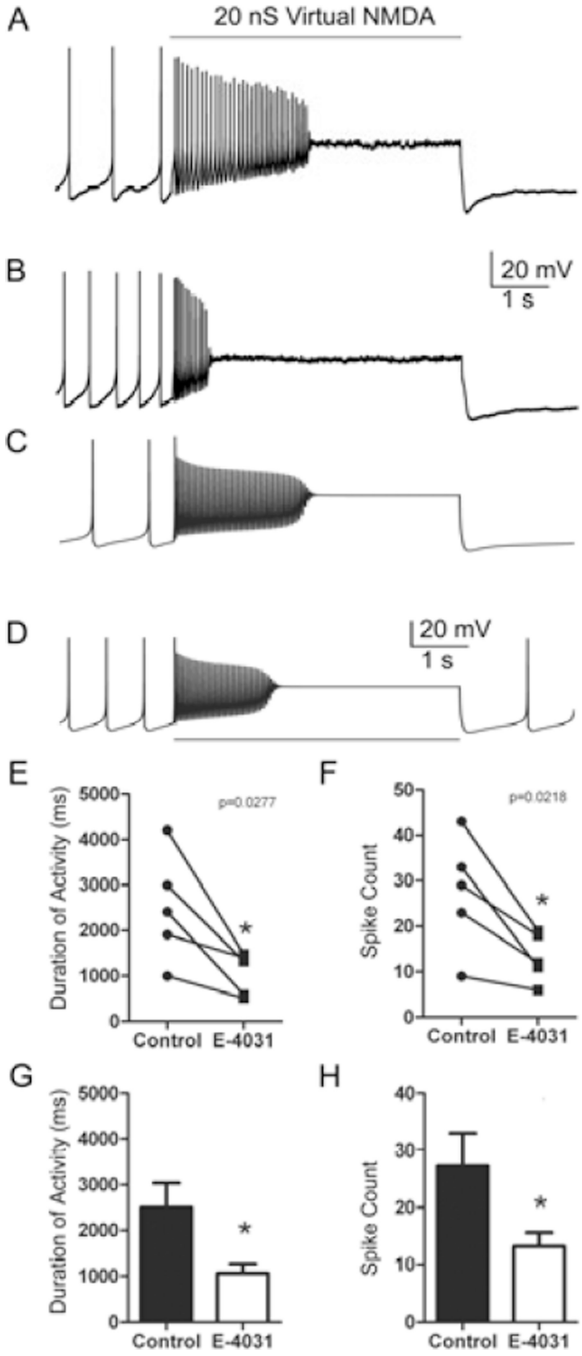

Figure 4.

E-4031 promoted depolarization block by virtual NMDA stimulation. (A and B) Representative whole-cell dynamic-clamp recordings of DA neurons stimulated with 20 nS of virtual NMDA current for 5 s to induce depolarization block before and after, respectively, superfusion with 10 μM E-4031. The horizontal line above the traces indicates virtual NMDA conductance application. (C and D) Simulated voltage traces for (C) control and (D) after simulated block of the ERG current (i.e. g_{ERG}=0). Summary of the effects of

10 μM E-4031 on (E and G) the duration and (F and H) the spike count from dynamic-clamp simulations of NMDA-induced bursting activity. *P<0.05.

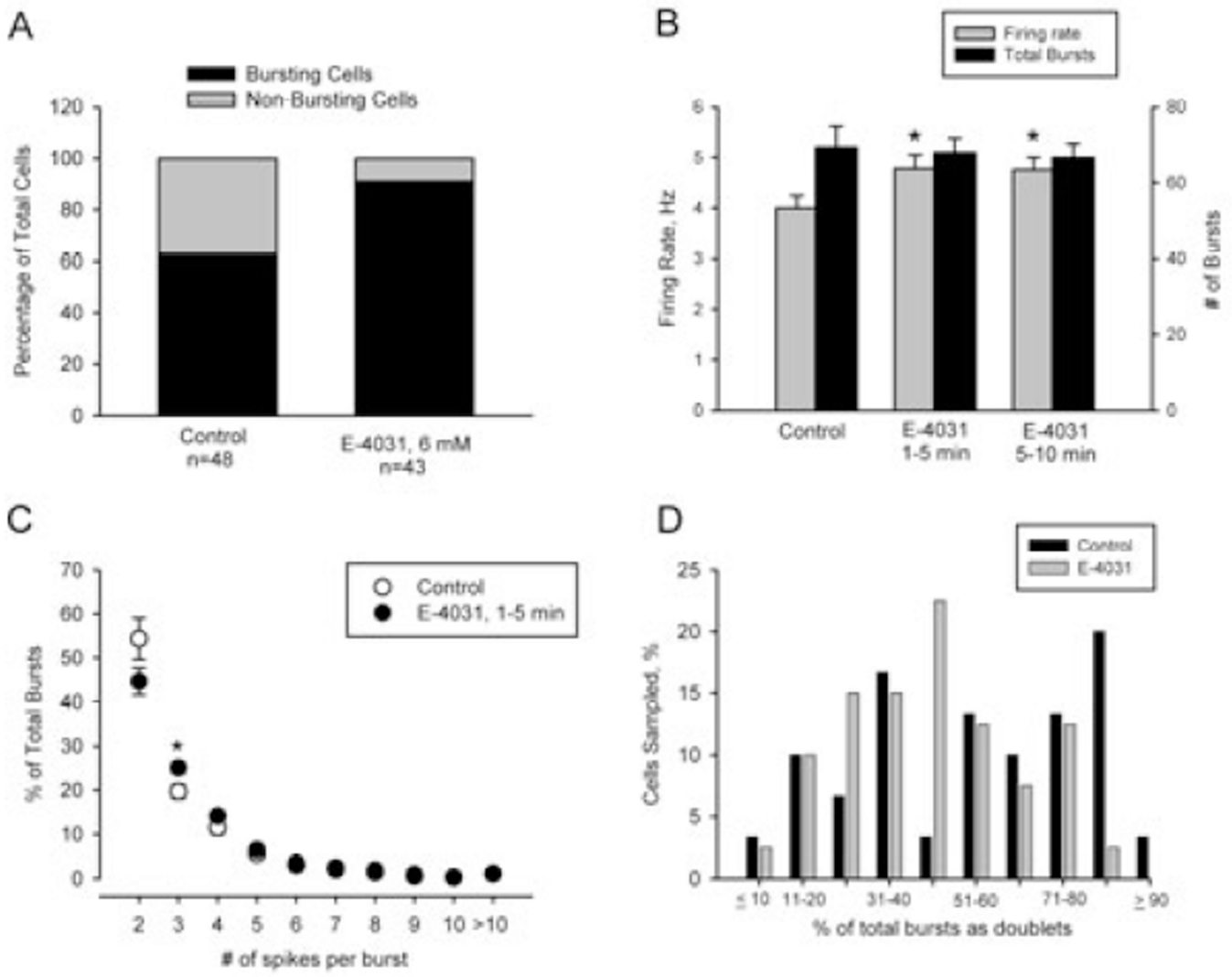

Figure 5.

Local application of E-4031 increased firing rate and burst firing *in vivo*. (A) The proportion of DA neurons encountered with a bursting and non-bursting discharge. In each experiment, control recordings were obtained using saline-filled pipettes prior to switching to electrodes containing saline + E-4031 (6 mM). Note the increased incidence of bursting cells recorded with electrodes containing the ERG blocker. (B) E-4031 increased spontaneous firing rate (grey bars) without changing the total number of bursts (black bars). The increase in firing rate induced by E-4031 could be attributed to the increased incidence of bursting activity. No significant differences were observed between the initial effects of the drug (1–5 minutes) and those observed after a longer duration exposure to E-4031. (C) E-4031 altered the composition of the burst, reducing the frequency of short bursts (two-spike or doublets) while increasing the incidence of three-spike bursts. (D) The frequency of two-spike bursts in control and E-4031-treated burst-firing cells. Note that the incidence of cells exhibiting > 80% of their bursts as doublets was diminished in E-4031-treated neurons.